

## Effect of ultrasonic waves on morphology and electrical treatment of graphene

**R Sabet Dariani, R Bakhshandeh, and H Haghi**  
Department of Physics- Chemistry, Alzahra University, Tehran, Iran

E-mail: R.Bakhshandeh@student.alzahra.ac.ir

(Received 05 November 2016 ; in final form 06 September 2017)

### Abstract

It is important to examine the factors that determine the properties of graphene. Various factors can affect the properties of graphene nano sheets. Understanding such factors can revolutionize the use of graphene. One such factor is ultrasonic waves, which have significant effects on graphene physical and chemical properties such as (electronic and optical). In this research, we studied the effect of ultrasonic waves with different power levels (35, 50, 360, and 420 W) on four graphene samples for 10 minute. So all the samples were fabricated by electrochemical exfoliation. In this method, ammonium sulfate nonorganic salt was used for producing solution and electrodes PT and graphite were used, where +10 volt was applied to the electrodes. Ultrasonic waves were used to homogenize the electrolyte for the samples. The samples were analyzed using scanning electron microscope (SEM) imaging and Fourier transform infrared spectroscopy (FTIR) spectroscopy. The I-V curves of the samples were measured after spraying on the glass substrate. Then, FTIR spectra and I-V characteristics were studied. Our results showed that the increase of ultrasonic power could cause some changes in the intensity of spectral FTIR and the conductivity of graphene sheets.

**Keywords:** graphene, electrochemical, ultrasonic wave, FTIR, SEM

### 1. Introduction

Graphene is an allotrope of carbon in the form of a hexagonal lattice with  $sp^2$  hybridization. It is a two-dimensional, atomic-scale, hexagonal lattice [1, 2]. The carbon-carbon bond length in graphene is about 0.142 nanometers. The single-layer graphene is the basis for carbon nanostructure formation. When stacked, they form 3D graphite with Van der Waals interaction and an interplanar spacing of 0.335 nm [3-6]. In statistical mechanics and quantum field theory, the Mermin-Wagner theorem states that the formation of 2D materials is impossible and that such materials are unstable; however, in 2004, Andre Geim and Konstantin Novoselov from Manchester University created such a material, showing that Mermin-Wagner theorem could not always be true [7]. Graphene has some particular magnetism and a theoretical specific surface area ( $2630 \text{ m}^2\text{g}^{-1}$ ), great mechanical properties (Young's modulus  $> 1 \text{ TPa}$ ), and high thermal conductivity ( $5000 \text{ W/mk}$ ), [8-10]. Due to its unique properties, graphene is desirable for designing the next-generation of electronic and optical components such as

Nano electronics devices, drug delivery, energy storage, solar cells, sensors and electronics and photonics as some examples of the graphene utilization [11-14]. There are many methods for the fabrication of graphene, such as micromechanical exfoliation, epitaxial growth on silicon carbide, chemical vapor deposition, photo reduction of graphene oxide, chemical reduction of graphene oxide, and Electrochemical Exfoliation [15-17]. In this research, four graphene samples were produced under equal conditions using electrochemical exfoliation. Then, the electrolytes of the samples were homogenized using ultrasonic waves with four different power levels (35, 50, 360, and 420 W) for 10 minute; they were dried under equal conditions. The bonds and dimensions of the samples were examined in relation to conductivity.

### 2. Characterization and equipment

Scanning Electron Microscopy (SEM) was used to view the surface of the samples (top view). Fourier transform infrared (FTIR) spectroscopy (TENSOR 27, Bruker) was utilized to determine the composite material.

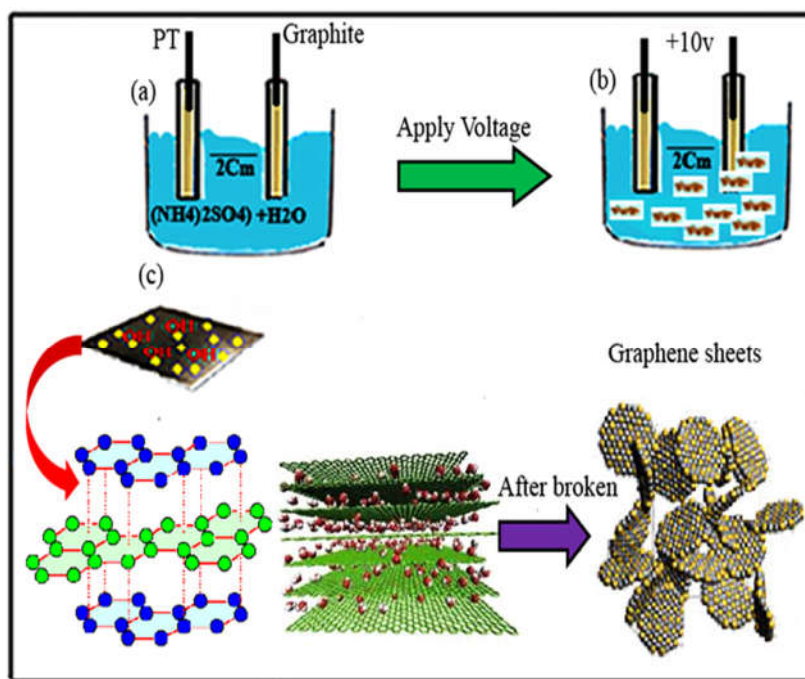


**Figure 1.** (color online) (a) Electrochemical setup. (b) Graphite exfoliation. (c) OH on the graphite electrode and broken bonds in the graphite structure.

### 3. Experimental

Electrochemical exfoliation of graphite was performed in aqueous inorganic salts, such as ammonium sulfate ((NH<sub>4</sub>)<sub>2</sub>SO<sub>4</sub>). 25 mL of distilled water and 0.165 g of ammonium sulfate were used to create the desired solution for the electrolysis process. Electrochemical exfoliation of graphite was accomplished in a two-electrode system using platinum as the counter and a graphite foil as the working electrode graphite and platinum, with each having 2\*2 cm<sup>2</sup> dimension. The distance between the electrodes was 2 cm and this distance was kept constant throughout the exfoliation process. After adjusting their distance, the electrodes were placed in a 0.05 molar ammonium sulfate solution. Platinum electrode tip was connected to the cathode and graphite electrode tip was connected to the anode. +10 V direct voltage was applied to the graphite electrode for 20 minutes, making graphite sheets swell and breaking the bonds between sheets and separating them. After 20 minutes, the four samples underwent 35, 50, 360, and 420 W ultrasonic treatment for 15 minutes. Subsequently, the samples were passed through a filter paper and dried at 80° C under equal conditions [18]. The electrolysis process is shown in figure 1. SEM imaging, FTIR spectroscopy, and output current were used to analyze the bonds and dimensions of the samples.

### 4. Results and dissection

**4. 1. FTIR spectrum** is one of the most important spectra used in the identification of the functional groups. figure 2 shows the FTIR spectrum of graphite and the created samples. In all four samples, C=C, C-O, and OH bonds were seen at 1600 cm<sup>-1</sup>, 1100 cm<sup>-1</sup>, and 3400 cm<sup>-1</sup>. FTIR spectrum showed the reduced presence

of oxygenated functional groups in the samples with the higher ultrasonic power. The presence of C=C and OH bonds was, respectively, due to the formation of aromatic rings and the breaking of bonds between water molecules. The presence of C-O was due to epoxy groups in graphene. A remarkable feature of the electrochemical exfoliation technique is that C=O, which is a reason for the presence of carbonyl groups, was not observed in the structure of graphene sheets [20]. This showed that electrochemical exfoliation was superior to other techniques.

### 4. 2. SEM images

Figure 3 illustrates the SEM images of the samples. A flat and continuous surface and less structural impurities were three important factors which determined the quality of the graphene layer. The samples were significantly different. The fabricated sample at low-power ultrasonic had larger than dimensions that the two samples created at the high-power ultrasonic. At higher power levels, stronger vibrations were applied to the samples, which caused graphene sheets to be broken further. Figure 4 illustrates the changes in the dimensions of graphene sheets with the increase in the ultrasonic power.

### 5. Spraying method

Spraying technique was used to measure the current passing through each sample. Spraying is one method used for examining micro particles. Deposition can be easily done at nanoscale using the spraying technique. To spray the samples, an air pump was used with 20 psi output pressure and a pressure regulator was set to one and a half turns, with a spraying speed of 0.01 ml/s. The

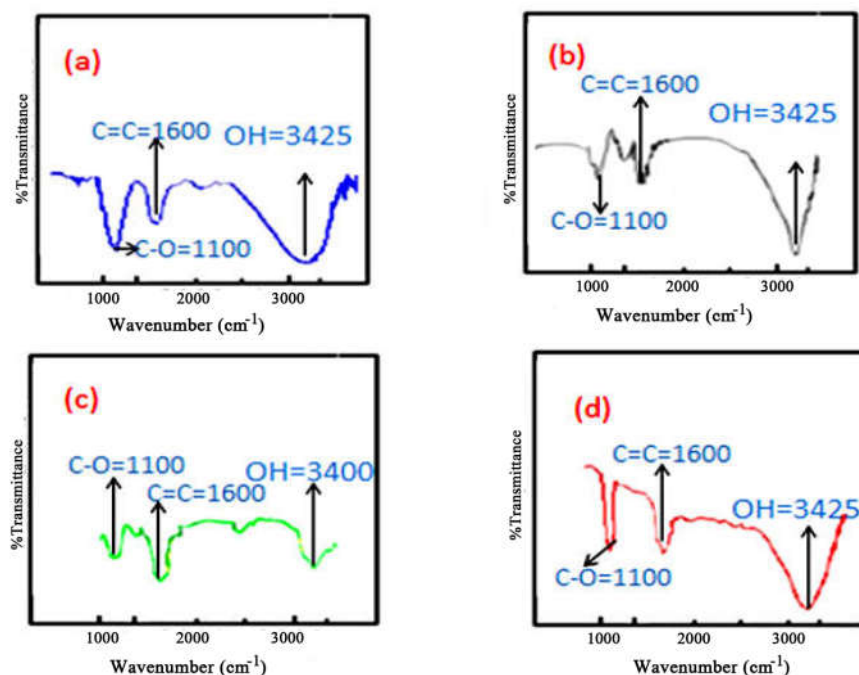


**Figure 2.** (color online) (a) FTIR of ultrasonic 35 W. (b) FTIR of ultrasonic 50 W. (c) FTIR of ultrasonic 360 W. (d) FTIR of ultrasonic 420 W.

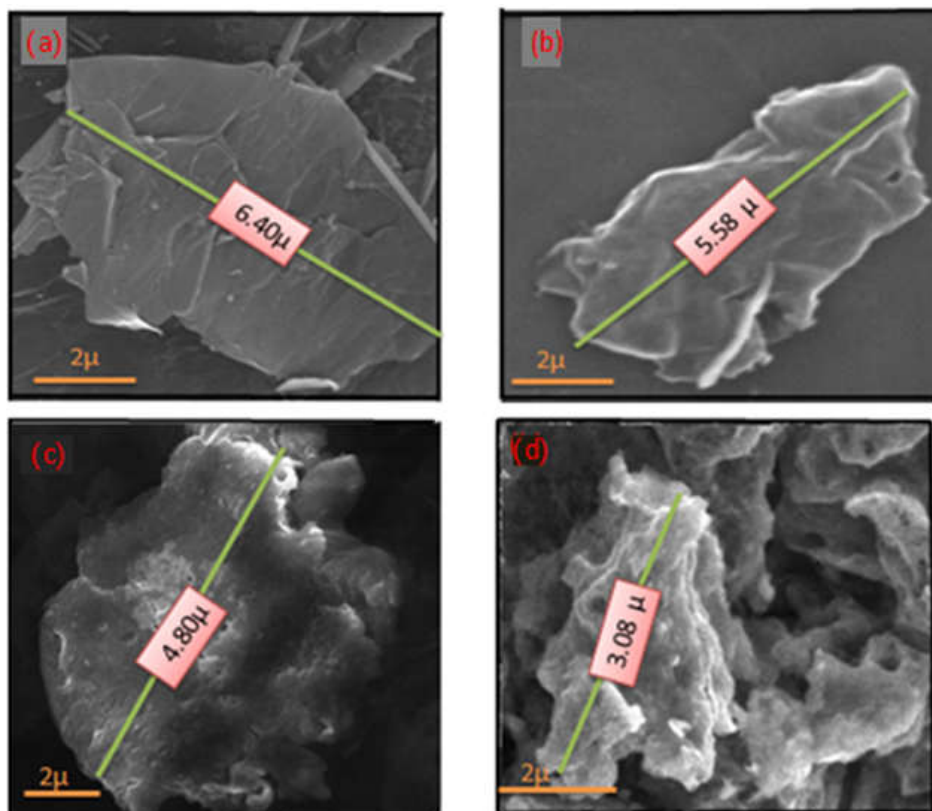


**Figure 3.** (color online) SEM image. (a) Graphene under the influence of ultrasonic 35 W. (b) Graphene under the influence of ultrasonic 50 W. (c) Graphene under the influence of ultrasonic 360 W. (d) Graphene under the influence of ultrasonic 420 W.

needle distance was set at 11.5 cm. 250 mg graphene powder was solved in 20 ml DMF; then this solution was sprayed on the Lamell surface with the dimensions of 1.5 cm<sup>2</sup>. The sample was cooled down to room temperature.

After cooling, copper wires were connected to both tips of the sample using the silver paste. When dried, the samples were placed in a circuit shown in figure 5 in order to measure their I-V.

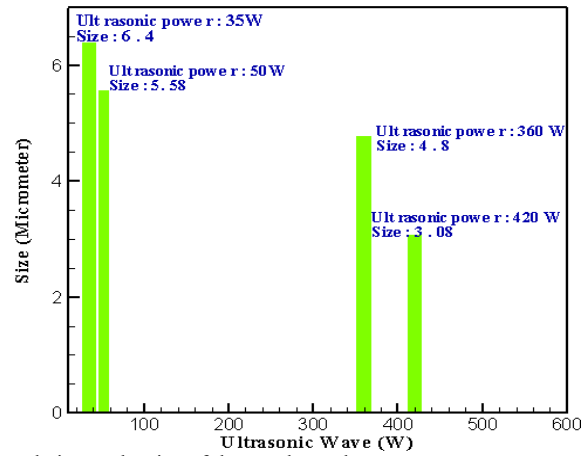


Figure 4. (color online) Ultrasonic relation to the size of the graphene sheets.

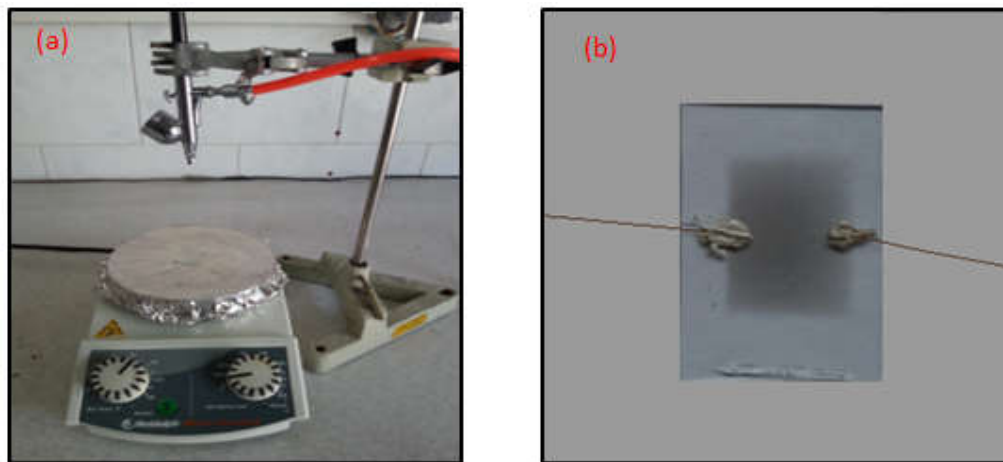


Figure 5. (color online) (a) Spray setup. (b) Graphene on the substrate.

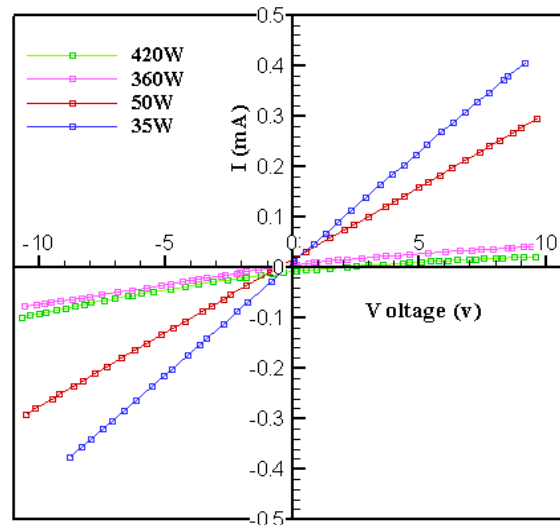
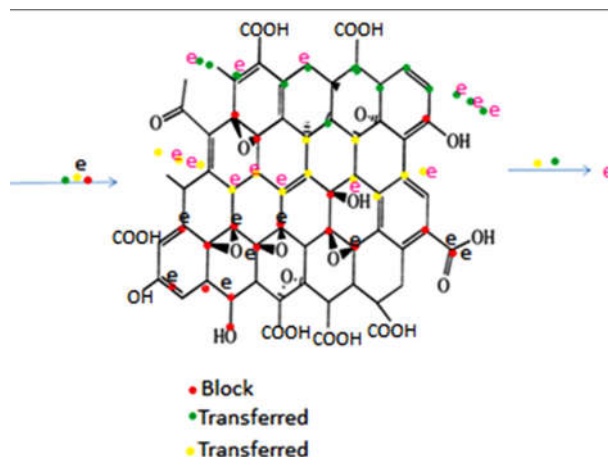


Figure 6. (color online) I-V behavior of four samples

### 6. I-v behavior

Changes in the I-V behavior of the four synthesized samples at 35, 50, 360, and 420 power levels are shown within the voltage range of  $[-10, +10]$ . Values from the I-V curves of the samples indicated the ohmic behavior and the resistivity obtained from the data was in the

order of kilo-ohm [20, 21]. It was found that the sample with the minimum ultrasonic power had the maximum resistance in comparison to other samples. With the increase of ultrasonic power, the resistance of samples was reduced, indicating the increase of conductivity in the samples. Four graphene samples were created using



**Figure 7.** Motion of electrons in the graphene sheets.

electrochemical exfoliation with 30, 50, 360, and 420 W ultrasonic. The properties of the samples showed that the increase in ultrasonic power caused the enhancement of conductivity. Moreover, the I-V curve of the samples followed Ohm's law and was linear. One of the main reasons for the enhanced conductivity as a result of the increased ultrasonic power was that, according to FTIR spectra, the presence of functional groups could be decreased as ultrasonic power is increased. This decrease in the number of functional groups around graphene rings could facilitate electron movement, the main cause of increased conductivity. In other words, reducing the nuisance variables in graphene nanosheets caused electrons to move more easily, thereby increasing conductivity. Figure 7 illustrates the fact that the red incident electron impinged on functional groups on its path and stops. However, yellow and green electrons stayed on their path on graphene rings without impinging

on the functional groups and continued to move by means of resonance within the structure of benzene rings; so they were measured as the sample current.

## 7. Conclusion

This study indicated that the produced graphene plates were highly affected by the external factors. To produce the graphene plates with higher quality, the intruder factors such as factor groups should be minimized. This study showed that the vibrations of ultrasonic waves could break the graphene plates and convert them into smaller dimensions. Specifying the external factors could a very important factor in determining the place of using graphene in the industry. Finding the factors which can increase the conductivity of graphene is very important and promoting this issue improves the place of graphene in the industry.

## References

1. S Narendar and S Gopalakrishnan, *Physica E Low-Dimensional Systems and Nanostructures* **42**, 5 (2010) 1601.
2. S Narendar, D R Mahapatra, and S Gopalakrishnan, *Computational Materials Science* **49**, 4 (2010) 734.
3. P Khaled, Z S Wu, R Li, X Liu, R Graf, X Feng, and K Müllen, *Journal of the American. Society* **136** (2014) 6083.
4. C Wu, Q Cheng, K Wu, G Wu, and Q Li, *Analytica Chimica Acta* **825** (2014) 26.
5. L Bing, X Zhang, P Xinghua *et al.*, *Royal Society of Chemistry Advances* **4**, 5 (2014) 2404.
6. C Kunfeng and D Xue, *Journal of Materials Chemistry A* **4**, 20 (2016) 7522.
7. K I Mikhail, *Materials Today* **10**, 1 (2007) 20.
8. T Prashant, C Ravi Prakash, M A Shaz, and O N Srivastava. *arXiv preprint arXiv:1310.7371*.
9. P Khaled, S Y Xinliang Feng, and K Müllen, *Synthetic Metals* **210** (2015) 123.
10. M Kasturi, R Geetha Bai, I B Abubakar, S M Sudheer, H N Lim, H-S Loh, N M Huang, C Hua Chia, and S Manickam, *International Journal of Nanomedicine* **10** (2015) 1505.
11. Q Mildred, K Spyrou, M Grzelczak, W R Browne, P Rudolf, and M Prato, *American Chemical Society Nano* **4**, 6 (2010) 3527.
12. L Sen, J Tian, L Wang, and X Sun, *Carbon* **49**, 10 (2011) 3158.
13. Y EunJoo, J Kim, E Hosono, H shen Zhou, T Kudo, and I Honma, *Nano Letters* **8**, 8 (2008) 2277.
14. P Michaela, A Kouloumpis, D Gournis, P Rudolf, and H Stamatis, *Sensors* **16**, 3 (2016) 287.
15. J Liu, L Cui, and D Losic, *Acta Biomaterialia* **9**, 12 (2013) 9243.
16. L Sen, J Tian, L Wang, and X Sun, *Carbon* **49**, 10 (2011) 3158.
17. M Roberto and C Gómez-Aleixandre, *Chemical Vapor Deposition* **19**, 10-11-12 (2013) 297.
18. R Bakhshandeh and A Shafiekhani, *Materials chemistry and physics* **212** (2018) 95.
19. Z Yonglai, L Guo, S Wei, Y He, H Xia, Q Chen, H Bo Sun, and F Shou Xiao, *Nano Today* **5**, 1 (2010) 15.
20. C Ji, B Yao, C Li, and G Shi, *Carbon* **64** (2013) 225.

21. J Changwook, P Nair, M Khan, M Lundstrom, and M A Alam, *Nano Letters* **11**, 11 (2011) 5020.  
22. L Xuesong, Y Zhu, Weiwei Cai, M Borysiak, B Han,

David Chen, R D Piner, L Colombo, and R S Ruoff, *Nano Letters* **9**, 12 (2009) 4359.